Reactions of substituted benzene anions with N and O atoms: Chemistry in Titan's upper atmosphere and the interstellar medium

Zhe-Chen Wang and Veronica M. Bierbaum

Reactions of substituted benzene anions with N and O atoms: Chemistry in Titan's upper atmosphere and the interstellar medium

Zhe-Chen Wang and Veronica M. Bierbaum
Department of Chemistry and Biochemistry, University of Colorado, Boulder, Colorado 80309, USA

The likely existence of aromatic anions in many important extraterrestrial environments, from the atmosphere of Titan to the interstellar medium (ISM), is attracting increasing attention. Nitrogen and oxygen atoms are also widely observed in the ISM and in the ionospheres of planets and moons. In the current work, we extend previous studies to explore the reactivity of prototypical aromatic anions (deprotonated toluene, aniline, and phenol) with N and O atoms both experimentally and computationally. The benzyl and anilinide anions both exhibit slow associative electron detachment (AED) processes with N atom, and moderate reactivity with O atom in which AED dominates but ionic products are also formed. The reactivity of phenoxide is dramatically different; there is no measurable reaction with N atom, and the moderate reactivity with O atom produces almost exclusively ionic products. The reaction mechanisms are studied theoretically by employing density functional theory calculations, and spin conversion is found to be critical for understanding some product distributions. This work provides insight into the rich gas-phase chemistry of aromatic ion-atom reactions and their relevance to ionospheric and interstellar chemistry. *Published by AIP Publishing.* [http://dx.doi.org/10.1063/1.4952454]

INTRODUCTION

The atmosphere of Titan has received increasing attention since the first flyby of the Cassini spacecraft more than ten years ago.[1–11] Various neutral and cationic species have been newly observed by the Ion Neutral Mass Spectrometer (INMS) and negative ions have been detected by the Cassini Plasma Spectrometer (CAPS).[12] These observations indicate that complex chemistry in Titan's upper atmosphere plays an important role in the formation of the thick aerosol layer.[2,13] The same chemistry may have occurred in the nitrogen-dominated atmosphere of early Earth $\sim 10^9$ years ago.[14] The key precursors leading to aerosols are likely to be *aromatic*.[2,13] It was unexpected that negatively charged molecules, whose existence was not previously considered, would be widely observed by CAPS in high altitudes of Titan's atmosphere.[2,3,12,15–18] Beginning in 2006, negative ions have also been detected in interstellar clouds, and six species, CN^-, C_3N^-, C_5N^-, C_4H^-, C_6H^-, and C_8H^-, have now been confirmed.[19–25] These observations suggest that anionic reactions may be important in the formation and distribution of species in the interstellar medium (ISM).[26,27] Cyclic aromatic molecules are ubiquitous throughout the ISM[2,28–31] and N and O atoms show high interstellar atomic abundance. An understanding of reactions between aromatic anions and atomic species can help to understand the formation and evolution of the ISM.

Experimental studies of the reactions of N and O atoms are challenging.[32] However, we have successfully studied the reactions of carbon chain anions (such as C_n^- and HC_n^-) and N-containing hydrocarbon chain anions (such as CH_2CN^-, CH_3CHCN^-, and $(CH_3)_2CCN^-$) with ground state atomic $N(^4S)$ and $O(^3P)$.[33,34] The reactions of C_n^- with N atoms

can form the N-containing carbon chain anions CN^-, C_3N^-, and C_5N^-, which have been observed in the ISM and in Titan's upper atmosphere.[3,19,23,24] The reaction rate constants of carbon chain anions with O atoms are approximately one order of magnitude larger than those with N atoms, and the neutral product CO is generated instead of C_nO^-.[34] Spin-forbidden processes have been discussed for the reactions of N-containing hydrocarbon chain anions with N and O atoms, and the importance of spin conservation and conversion on the reactions of interstellar species of high multiplicity such as $N(^4S)$ and $O(^3P)$ has been recognized.[33]

Recently, we also studied the reactions of phenide ($C_6H_5^-$), pyridinide ($C_5H_4N^-$), 1,2-, 1,3-, and 1,4-diazinide ($C_4H_3N_2^-$), and 1,3,5-triazinide ($C_3H_2N_3^-$) with ground state $N(^4S)$ and $O(^3P)$ atoms. The major reaction channel of these azine anions with N and O atoms is associative electron detachment to produce electrons and neutral products. The reactions of N atoms with azine anions (reaction rate constants on the order of 10^{-10} cm^3 s^{-1}) are generally faster than those with the carbon chain anions.[33,34] Additionally, the reactions of azine anions with O atoms are $\sim$2-5 times faster than those with N atoms and show complicated and intriguing ionic product patterns.[35] We have also recently reported the reactions of OCN^- with N and O atoms and determined that the processes are immeasurably slow.[36] In this paper, we investigate the reactions of benzyl, anilinide, and phenoxide anions with N and O atoms experimentally and theoretically. The major reaction channel for benzyl and anilinide anions with N and O atoms is associative electron detachment (AED) to produce electrons and neutral products; in the reactions with O atoms, ionic products are also observed. However, the reactions of phenoxide anions are strikingly different: There is no reaction with N atoms, and the major reaction channels with O atoms are ion generating path-

ways. This behavior dramatically contrasts with previously studied reactions of carbon-containing aromatic species with O atoms. Density functional theory (DFT) calculations are used to study the energies of the reactants, ion complexes, transition states, and products to examine the reaction mechanisms in detail as well as to elucidate the spin conversion processes in the ion-atom reactions.

EXPERIMENTAL AND COMPUTATIONAL METHODS

Measurements of the reaction rate constants and product distributions were made using the tandem flowing afterglow-selected ion flow tube (FA-SIFT) at the University of Colorado, Boulder. This instrument has been described elsewhere,[37,38] and only the salient details for these experiments will be discussed here. Ions are generated using electron and chemical ionization methods in the source flow tube. A small flow of NH_3 entrained in helium buffer gas is passed over a rhenium filament to generate NH_2^-, which further reacts with neutral molecules to form the deprotonated species

$$NH_2^- + HA \rightarrow NH_3 + A^-. \quad (1)$$
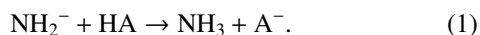
The anions are mass-selected with the SIFT quadrupole mass filter and injected into the reaction flow tube. They are then entrained in helium buffer gas (0.37 Torr, ~200 std cm^3 s^{-1}) at 298 K and thermalized by multiple collisions. The ion-neutral reaction is initiated by adding N or O atoms to the flow tube through an inlet positioned 70 cm upstream of the sampling orifice. Reactant and product ions are monitored with a quadrupole mass filter coupled with an electron multiplier. Microwave discharge flow techniques are used to generate N and O atoms in their ground states, which are well-established methods for studying the reactions of ions with atoms using the FA-SIFT.[33–35,39–46]

Figure 1 is the sample titration plot showing the logarithm of the intensity of benzyl anion ($C_6H_5CH_2^-$) *versus* the flow of NO. At point A, N_2 is introduced into the flow tube with the microwave discharge off and no reaction is evident. After ignition of the discharge, N atoms are formed, and the intensity of the ions decreases slightly to the lower value at point B due to the reaction with N atoms. When NO is added to the system, N reacts with NO to generate O, and the increased depletion of the ion signal indicates the occurrence of the faster reaction, $C_6H_5CH_2^- + O$ (region C). The intersection point D represents the endpoint of the titration; the flow of NO at this point is equal to both the N atom flow at the beginning of the titration as well as the O atom flow at the endpoint. Further addition of NO beyond the endpoint, region E, causes the recovery of the ion signal, because O atoms are removed by reaction with NO to form NO_2; subsequent reaction of NO_2 with O forms O_2 and regenerates NO. The ion loss, the atom flow rate, and other experimental parameters are used to determine the pseudo-first order reaction rate constants.

DFT calculations using the *Gaussian* 09 program[47] are employed to study the reactions of the anions with N and O atoms. These calculations involve geometry optimization of various reaction intermediates and transition states. Transition state optimizations are performed using either the Berny
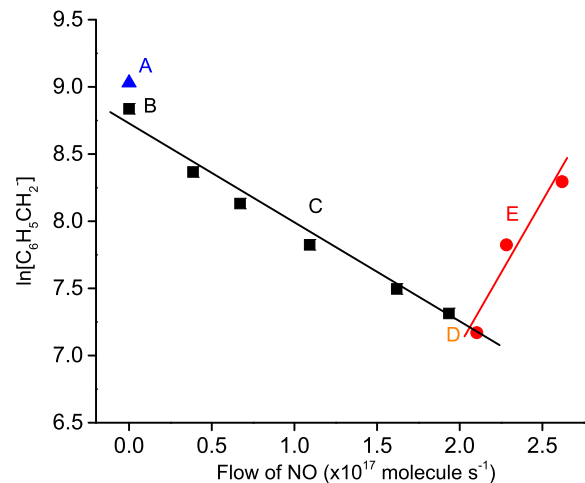

FIG. 1. Titration plot for the reaction of benzyl anion ($C_6H_5CH_2^-$) with N and O atoms. Point A, microwave discharge off; point B, microwave discharge on; region C, coexistence of N and O atoms; point D, titration endpoint; region E, coexistence of NO and O_2.

algorithm[48] or the synchronous transit-guided quasi-Newton (STQN) method.[49] For most cases, an initial estimated structure of the transition state is obtained through relaxed potential energy surface (PES) scans using an appropriate internal coordinate. Vibrational frequencies are calculated to confirm that the reaction intermediates have all positive frequencies and transition state species have only one imaginary frequency. Intrinsic reaction coordinate (IRC) calculations[50,51] are also performed so that a transition state connects two appropriate local minima in the reaction paths. The hybrid B3LYP exchange–correlation functional[52] is adopted. A Gaussian basis set 6-311++G(d,p) is used.[53,54] Test calculations indicate that basis set superposition error (BSSE) is negligible, and therefore BSSE is not taken into consideration. The zero-point vibration corrected energies (ΔE_{zpe}) are reported in this study. Cartesian coordinates, electronic energies, and vibrational frequencies for all of the optimized structures are available by request to the authors.

RESULTS AND DISCUSSION

Reactions with N atoms

The rate constants for reactions of the benzyl, anilinide, and phenoxide anions with N(^{4}S) and O(^{3}P) atoms are summarized in Table I. In parallel with the reaction of phenide anion, reaction (2), the dominant process for the reactions of benzyl and anilinide anions with N atoms is associative electron detachment (AED) to form electrons and neutral products, reactions (3) and (4). No ionic products are detected. The phenoxide anion is unreactive with N atom, reaction (5). The superscript numbers indicate the spin multiplicity of the species
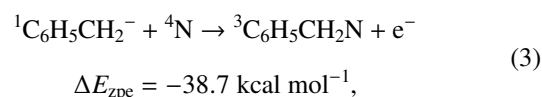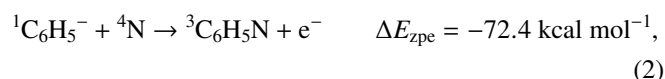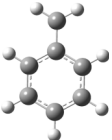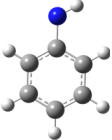
$$^1C_6H_5^- + {}^4N \rightarrow {}^3C_6H_5N + e^- \qquad \Delta E_{zpe} = -72.4 \text{ kcal mol}^{-1},$$
$$(2)$$

$$^1C_6H_5CH_2^- + {}^4N \rightarrow {}^3C_6H_5CH_2N + e^-$$
$$\Delta E_{zpe} = -38.7 \text{ kcal mol}^{-1},$$
$$(3)$$
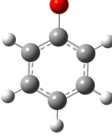
TABLE I. Reactions of benzyl, anilinide, and phenoxide anions with N and O atoms studied with FA-SIFT.

	N			O		
	$k_{exp}(N)^a/10^{-10} cm^3 s^{-1}$	AED[b]	Ionic products[c]	$k_{exp}(O)^a/10^{-10} cm^3 s^{-1}$	AED[b]	Ionic products[c]
$C_6H_5CH_2^-$ (benzyl)	0.65	1.0	N.D.[d]	1.5	0.90	$C_6H_5CHO^- + H$
$C_6H_5NH^-$ (anilinide)	0.13	1.0	N.D.[d]	4.4	0.85	$C_6H_5NO^- + H$ (0.45) $C_6H_4N^- + H_2O$ (0.40) $C_6H_5O^- + NH$ (0.15)
$C_6H_5O^-$ (phenoxide)	<0.10	N.A.[d]	N.D.[d]	3.6	<0.1	$C_5H_5O^- + CO$ (0.3) $C_6H_4O_2^- + H$ (0.4) $C_5H_5^- + CO_2$ (0.1) $C_4H_5^- + 2CO$ (0.2)

[a]The total error is estimated to be ±50%.
[b]The branching fractions for associative electron detachment (AED) are obtained by comparing the decrease of the parent ion signal with the intensity of total product ion signals (estimated error ±10%).
[c]Branching fractions for ionic product distributions are given in parentheses.
[d]N.D. indicates not detected, N.A. indicates not applicable.

$$^1C_6H_5NH^- + {}^4N \rightarrow {}^3C_6H_5NHN + e^-$$
$$\Delta E_{zpe} = -22.9 \text{ kcal mol}^{-1}, \quad (4)$$

$$^1C_6H_5O^- + {}^4N \rightarrow {}^3C_6H_5ON + e^-$$
$$\Delta E_{zpe} = +10.0 \text{ kcal mol}^{-1}. \quad (5)$$
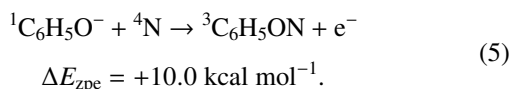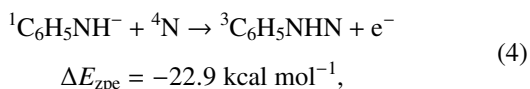
These AED processes are relevant to the chemistry of Titan's atmosphere, because it has been shown that nitrogen chemistry greatly influences the distribution of aromatic species in this environment.[55,56] Moreover, the balance of the neutral and charged species is affected as AED converts the identity of the negative charge carriers from ions to free electrons and neutral molecules. The rate constants for the reactions of benzyl and anilinide anions with N atoms are smaller than those of azine anions with N atoms but similar to N-containing hydrocarbon chain anions with N atoms.[33,35]
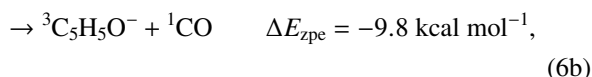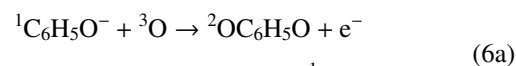
Computations employing the DFT method show that the AED processes for the reactions of N atom with $C_6H_5^-$, $C_6H_5CH_2^-$, and $C_6H_5NH^-$ are exothermic (reactions (2)–(4)). The rate constant for reaction of $C_6H_5^-$ with N atom is $1.8 \pm 0.9 \times 10^{-10}$ cm^3 s^{-1}, which is larger than those of $C_6H_5CH_2^-$ and $C_6H_5NH^-$ ($6.5 \pm 3.3 \times 10^{-11}$ and $1.3 \pm 0.7 \times 10^{-11}$, respectively). In contrast, the reaction of $C_6H_5O^- + {}^4N$ to form the AED products ($^3C_6H_5ON + e^-$ reaction (5)) is endothermic, and experimentally the reactivity is below our detection limit of 1.0×10^{-11} cm^3 s^{-1}. The experimental and computational results strongly indicate that, for the AED reactions with N atoms, the more exothermic reactions are faster. A similar observation has been reported previously.[43] The AED processes result in neutral molecules and electrons; the highly exothermic reaction 2 suggests that subsequent fragmentation of the neutral product $^3C_6H_5N$ can occur to form small neutral interstellar species.

Reactions with O atoms

The reaction of phenoxide anions with O atoms

The reaction of phenoxide anions with O atoms exhibits an extremely low AED branching fraction. This fraction is lower than ~10% (Table I), and ionic species dominate the product channels. This reaction is complex because various ionic products are observed experimentally (Table I and Figure 2): $C_5H_5O^-$, $C_6H_4O_2^-$, $C_5H_5^-$, and $C_4H_5^-$, corresponding to the formation of the neutral products CO, H, CO$_2$, and 2 CO, respectively (Figure 2). The zero-point vibration corrected reaction energies (E_{zpe}), determined by DFT calculations, are shown in reaction (6)

$$^1C_6H_5O^- + {}^3O \rightarrow {}^2OC_6H_5O + e^-$$
$$\Delta E_{zpe} = -1.2 \text{ kcal mol}^{-1}, \quad (6a)$$

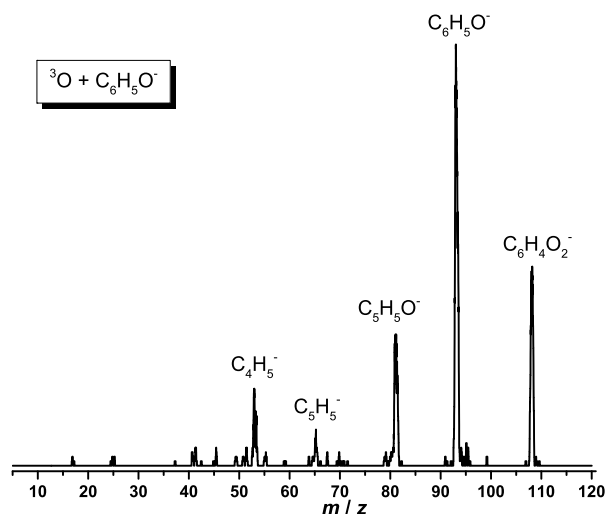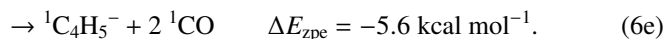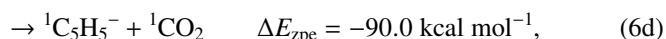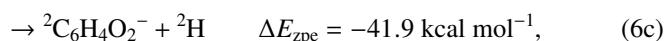$$\rightarrow {}^3C_5H_5O^- + {}^1CO \quad \Delta E_{zpe} = -9.8 \text{ kcal mol}^{-1}, \quad (6b)$$

FIG. 2. The ionic product distribution for the reaction of phenoxide anion ($C_6H_5O^-$) with O atoms is shown in this mass spectrum.

$$\rightarrow {}^2C_6H_4O_2{}^- + {}^2H \qquad \Delta E_{zpe} = -41.9 \text{ kcal mol}^{-1}, \qquad (6c)$$

$$\rightarrow {}^1C_5H_5{}^- + {}^1CO_2 \qquad \Delta E_{zpe} = -90.0 \text{ kcal mol}^{-1}, \qquad (6d)$$

$$\rightarrow {}^1C_4H_5{}^- + 2\,{}^1CO \qquad \Delta E_{zpe} = -5.6 \text{ kcal mol}^{-1}. \qquad (6e)$$

The reaction rate constant of $C_6H_5O^- + {}^3O$ is $3.6 \pm 1.8 \times 10^{-10}$ cm^3 s^{-1}, which is more than an order magnitude larger than the reaction rate constant for N atoms ($<0.10 \times 10^{-10}$ cm^3 s^{-1}). Based on our experimental observations, the product channels of ${}^2C_6H_4O_2{}^- + {}^2H$ (reaction (6c)) and

${}^3C_5H_5O^- + CO$ (reaction (6b)) are the dominant reaction pathways. The formation of carbon monoxide is not surprising since CO is very stable and the formation of CO has also been reported in the reactions of $C_n{}^-$, $HC_n{}^-$, $C_6H_5{}^-$, and c-$C_5H_4N^-$ with O atoms.[34,35] The loss of H atom from the interaction of O atom with $C_6H_5O^-$ is also an interesting process, which suggests the possible facile transformation of aromatic hydrocarbons to hydrogen-poor carbon species under some oxygen rich interstellar regions such as bowl shocks around stars.

The formation of two major products ${}^2C_6H_4O_2{}^- + {}^2H$ and ${}^3C_5H_5O^- + CO$ from the reaction of $C_6H_5O^-$ with ${}^3O$ atom on the triplet PES is shown in Figure 3. Three encounter complexes can be readily formed via the approach of ${}^3O$ atom to $C_6H_5O^-$, while the $O \cdot C_6H_5O^-$ isomers (**1** and **3** in Figure 3) are more favorable. The addition of O atom to $C_6H_5O^-$ is associated with an energy release which favors the evaporation of ${}^2H$ atom to generate ${}^2C_6H_4O_2{}^-$ (**1** → **1/2** → **2** → **2/P1** → **P1**). This reaction channel is overall barrierless and agrees well with our experimental observations. The stabilization energy gained in the first encounter step can also initiate a ring-opening reaction pathway (**3** → **3/4** → **4** → **4/5** → **5**), which can lead to the formation of the low-lying intermediate possessing the CO moiety (intermediate **5**, -49.8 kcal mol^{-1}). From **5**, the evaporation of CO is straightforward to generate ${}^3C_5H_5O^- + CO$ (**P2**). The overall barrier for the reaction channel that generates ${}^3C_5H_5O^- + CO$ (**P2**, -9.8 kcal mol^{-1}) is higher than that for ${}^2C_6H_4O_2{}^- + {}^2H$ (**P1**, -41.9 kcal mol^{-1}), which is consistent with the

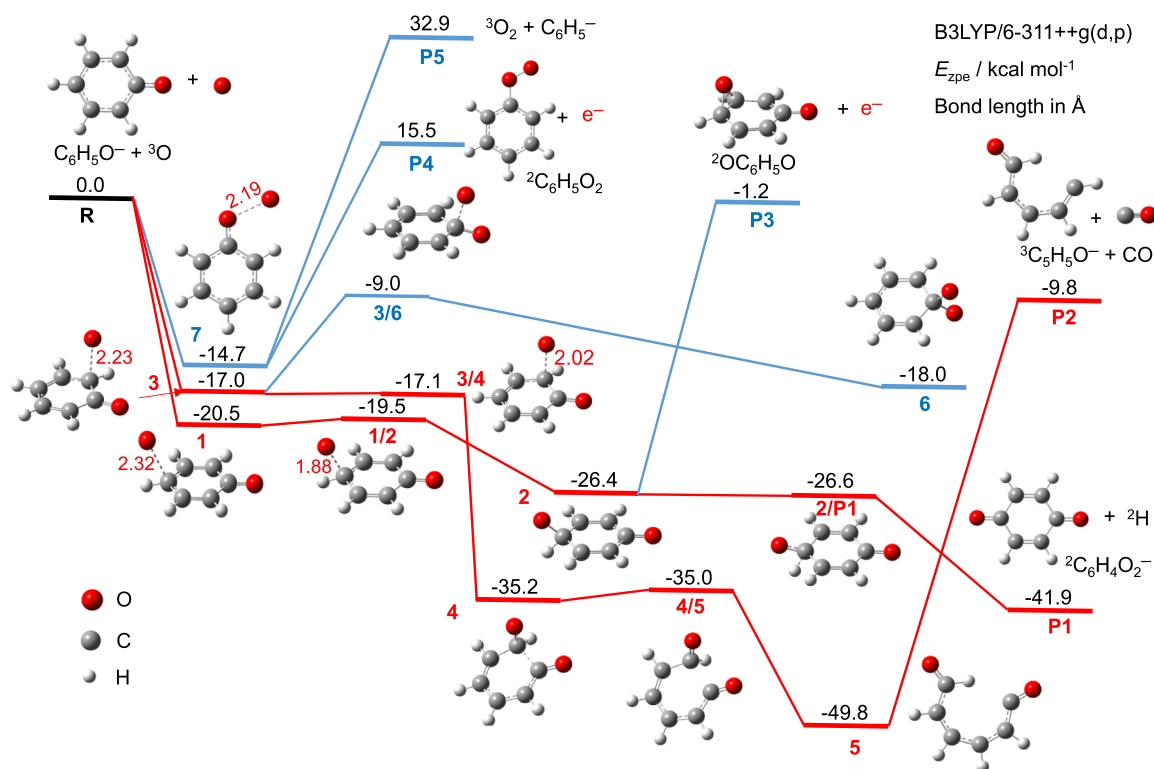
FIG. 3. Potential energy surfaces for the reaction of phenoxide ($C_6H_5O^-$) with ${}^3O$ on the triplet surface. The profiles are plotted for zero-point vibration corrected energies (E_{zpe}, kcal mol^{-1}) relative to the energy of the entrance channel. The intermediates and transition states are denoted in bold as **n** and **n1/n2**, respectively, and the products are denoted in bold as **Pn**. Some key bond lengths are given in Å. Red lines are barrierless reaction pathways. Blue lines are endothermic or high barrier reaction pathways.

lower product abundance of **P2** ($\sim$30%) relative to that of **P1** ($\sim$40%). From intermediate **2**, the AED process to generate an electron and the neutral $^2OC_6H_5O$ (**P3**) is only slightly exothermic (-1.2 kcal mol^{-1}). Considering that the accuracy of our calculations is $\sim\pm4$ kcal mol^{-1}, it is not possible to confirm this AED process as a favorable reaction channel. The direct formation of $^2C_6H_5OO + e^-$ (**P4**) from the $^3C_6H_5OO^-$ encounter complex (isomer **7**) is endothermic ($+15.5$ kcal mol^{-1}) and cannot occur under our experimental conditions. Considering the complexity of this reaction, there may be other pathways for the exothermic AED processes, which contribute less than 10% branching fraction. One might expect that the stable $C_6H_5^-$ can be formed as a product. However, the formation of $C_6H_5^- + {}^3O_2$ is endothermic by $+32.9$ kcal mol^{-1} and experimentally we do not observe any signal corresponding to the formation of $C_6H_5^-$. From isomer **3**, a stable intermediate **6** (-18.0 kcal mol^{-1}) containing the CO_2 moiety may be formed via the O atom transfer between neighboring C atoms (**3 → 3/6 → 6**). The intermediate **6** does not favor the formation of the CO_2 product because the C–C bond cleavage in **6** introduces barriers much higher than the energy of the entrance channel.

According to our calculations, the direct formation of the two minor products $^3C_5H_5^- + CO_2$ and $^3C_4H_5^- + 2$ CO on the triplet PES is unlikely, because there are high energy barriers between the reactants and the products. However, they can be formed easily on the singlet PES via a curve crossing. Figure 4 shows the possible reaction pathways for the formation of $C_5H_5^- + CO_2$ and $C_4H_5^- + 2$ CO on the singlet PES. The encounter complex **8** (-57.2 kcal mol^{-1}) on the singlet PES possesses very similar structure as **4** (-35.2 kcal mol^{-1}, triplet PES) but much lower energy, indicating the existence of a crossing point. From intermediate

8, the formation pathways of $C_5H_5^- + CO_2$ and $C_4H_5^- + 2$ CO are barrierless and energetically favorable on the singlet PES (Figure 4). The formation of the very stable CO_2 product involves an oxygen transfer and simultaneous C–C bond cleavage (**8 → 8/9 → 9**), leading to the formation of a stable seven-membered ring intermediate **9**. Then the elimination of a CO moiety from the ring causes the formation of a very stable five-membered ring intermediate **10** $[C_5H_5\text{–}CO_2]^-$ with a CO_2 side group (**9 → 9/10 → 10**). The direct evaporation of CO_2 from **10** leads to the formation of the final products $C_5H_5^- + CO_2$ (**P6**). From intermediate **8**, the hydrogen transfer between two carbon atoms to form –(CO)$_2$– is also feasible (**8 → 8/11 → 11**). And the consecutive loss of the two CO units to form the $C_4H_5^- + 2$ CO (**P7**) is overall barrierless. One may note that the formation of $C_5H_5^- + CO_2$ (**P6**) is energetically much more favorable than $C_4H_5^- + 2$ CO (**P7**). However, for spin forbidden reactions, the rate limiting step is the spin conversion process at the crossing point. This factor likely causes the similar product distributions for these reaction channels.

The reaction of O atoms with anilinide anions

Three ionic products have been observed for the reaction of anilinide ($C_6H_5N^-$) with O atom (Table I), reaction (7). According to our calculations, all three products can be formed on the triplet PES, which is shown in Figure 5; all three reaction pathways are overall barrierless. The formation of $^2C_6H_5NO^- + {}^2H$ (**P8**) is exothermic by 47.0 kcal mol^{-1}, which is the most favorable reaction channel. The formation of $^3C_6H_4N^- + H_2O$ (**P9**) is less exothermic than that of $^2C_6H_5O^- + {}^2NH$ (**P10**). However, the overall barrier of the latter (transition state **16/19**, -15.5 kcal mol^{-1}) is higher,

$C_6H_5O^- + {}^1O$
63.4
R1

$C_6H_5O^-$
$+ {}^3O$
0.0
R

B3LYP/6-311++g(d,p)

E_{zpe} / kcal mol^{-1}

CP

-17.0
3

3/4
-17.1

-35.2
4

8/9
-49.8

-57.2
8

-56.0
8/11

-74.3
9

-84.7
11

11/12
-27.9

9/10
-45.2

-33.7
12

-5.6
P7

$C_4H_5^-$

-93.6
10

$C_5H_5^-$

-90.1
P6

● O
● C
• H
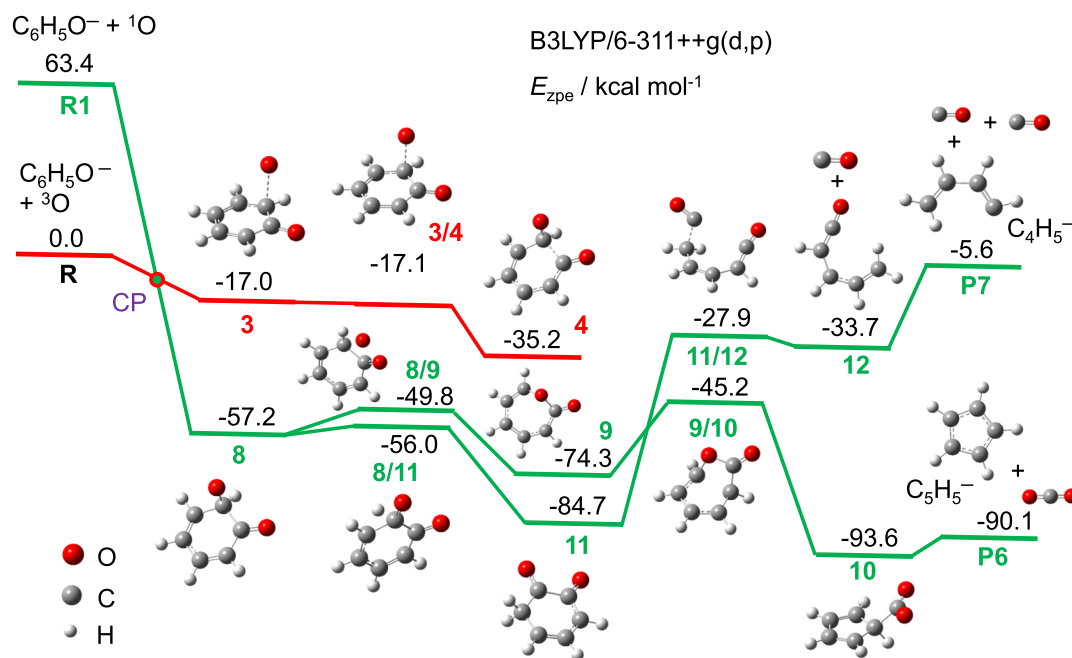
FIG. 4. Potential energy surfaces for the reaction of phenoxide ($C_6H_5O^-$) with O on the singlet surface. The profiles are plotted for zero-point vibration corrected energies (E_{zpe}, kcal mol^{-1}) relative to the energy of the triplet entrance channel. The intermediates and transition states are denoted in bold as ***n*** and ***n*1/*n*2**, respectively, and the products are denoted in bold as **P*n***. The possible crossing point is denoted as **CP**. The green lines are singlet PES and the red line is the triplet PES.
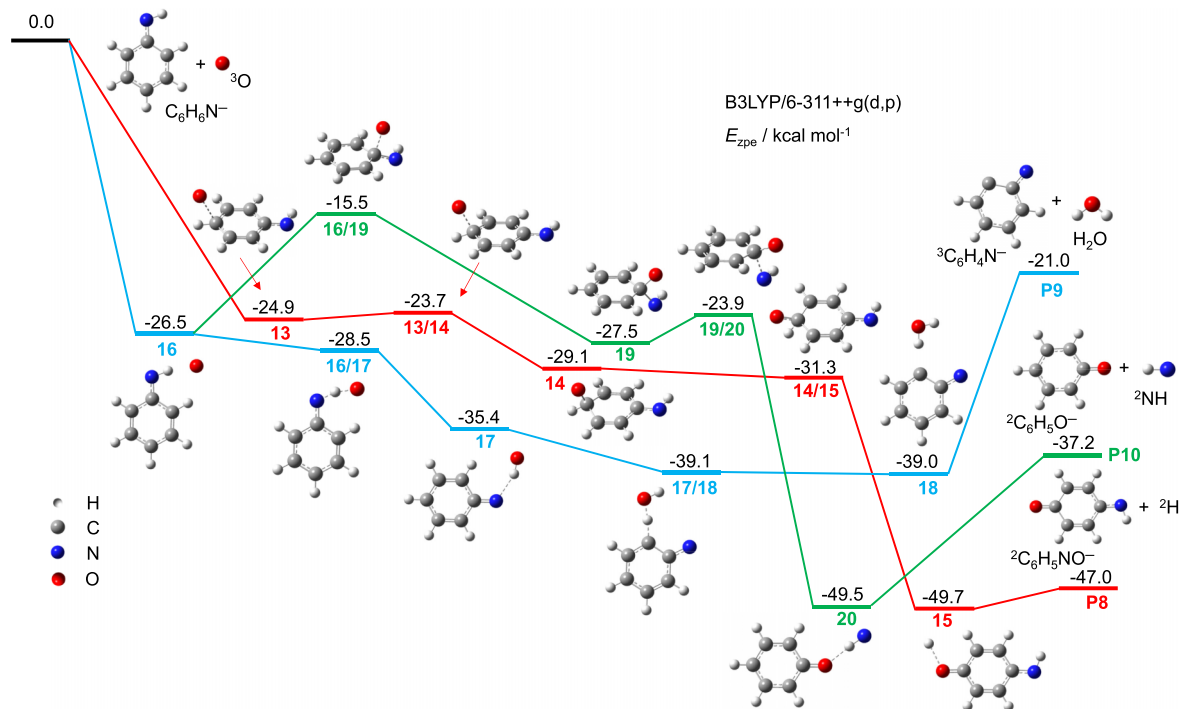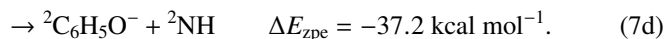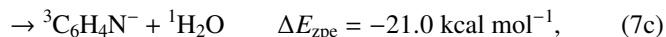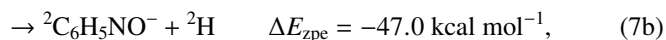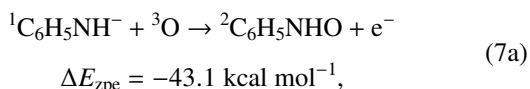
FIG. 5. Potential energy surfaces for the reaction of anilinide ($C_6H_5NH^-$) with O on the triplet surface. The profiles are plotted for zero-point vibration corrected energies (E_{zpe}, kcal mol^{-1}) relative to the energy of the triplet entrance channel. The intermediates and transition states are denoted in bold as **n** and **n1/n2**, respectively, and the products are denoted in bold as **Pn**. Different reaction pathways are denoted with different colors.
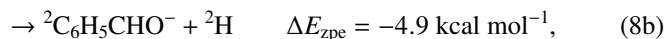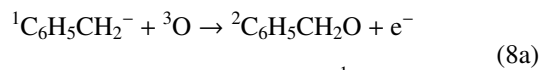
leading to the lower abundance of $^2C_6H_5O^- + {}^2NH$ (**P10**). Complicated H atom transfer processes are necessary for the formation of $^3C_6H_4N^- + H_2O$ (**P9**). The calculated results agree well with the experimental observation

$$^1C_6H_5NH^- + {}^3O \rightarrow {}^2C_6H_5NHO + e^-$$

$$\Delta E_{zpe} = -43.1 \text{ kcal mol}^{-1}, \tag{7a}$$

$$\rightarrow {}^2C_6H_5NO^- + {}^2H \qquad \Delta E_{zpe} = -47.0 \text{ kcal mol}^{-1}, \tag{7b}$$

$$\rightarrow {}^3C_6H_4N^- + {}^1H_2O \qquad \Delta E_{zpe} = -21.0 \text{ kcal mol}^{-1}, \tag{7c}$$

$$\rightarrow {}^2C_6H_5O^- + {}^2NH \qquad \Delta E_{zpe} = -37.2 \text{ kcal mol}^{-1}. \tag{7d}$$

The reaction of O atoms with benzyl anions

The reaction of benzyl anion ($C_6H_5CH_2^-$) with O is rather simple. Only one ionic product $^2C_6H_5CHO^-$ has been observed, which is a straightforward O addition and H loss reaction pathway (Figure 6). This ionic product reaction channel (**P12**, -4.9 kcal mol^{-1}, reaction (8b)) is much less favorable than the AED process to form $^2C_6H_5CH_2O + e^-$ (**P11**, -53.5 kcal mol^{-1}, reaction (8a)). The photoelectron spectrum of the $C_6H_5CHO^-$ radical anion was recently reported by Bowen and co-workers,[57] and the electron affinity of ground state C_6H_5CHO is found to be 8.1 kcal mol^{-1}. Thus, the formation of $^1C_6H_5CHO + H + e^-$ will be endothermic by about 3.2 kcal mol^{-1}, indicating that the consecutive loss of an electron from the product H^- is not feasible and observation of the ionic product $^2C_6H_5CHO^-$ is reasonable. The electron affinity of H atom is 17.4 kcal mol^{-1}, much higher than that of C_6H_5CHO. Therefore another possible reaction pathway can be the formation of $C_6H_5CHO + H^-$. However, the formation of the singlet product C_6H_5CHO is a spin-forbidden process,

and the formation of triplet $C_6H_5CHO + H^-$ is endothermic by 4.7 kcal mol^{-1} (**P13**, reaction (8c))

$$^1C_6H_5CH_2^- + {}^3O \rightarrow {}^2C_6H_5CH_2O + e^-$$

$$\Delta E_{zpe} = -53.5 \text{ kcal mol}^{-1}, \tag{8a}$$

$$\rightarrow {}^2C_6H_5CHO^- + {}^2H \qquad \Delta E_{zpe} = -4.9 \text{ kcal mol}^{-1}, \tag{8b}$$

$$\rightarrow {}^3C_6H_5CHO + {}^1H^- \qquad \Delta E_{zpe} = +4.7 \text{ kcal mol}^{-1}. \tag{8c}$$

Relevance to Titan's upper atmosphere and the interstellar medium

Negative ion spectra from the Cassini Plasma Spectrometer show a high abundance/strong peaks of m/z 90–95 species in the upper atmosphere of Titan.[58,59] Benzene is considered to be the key precursor species to form aromatic aerosols.[13] The harsh environment of Titan's upper atmosphere is caused by high energy photons, electrons, and ions. The benzene derivatives might be easily synthesized under such a reactive environment. The anions of deprotonated toluene, phenol, and aniline occur at m/z 92, 94, 93, respectively, and thus are possible candidates for the anions detected in the mass range of 90–95. Furthermore, the low reactivity of these ions with N atoms indicates their possible persistence in the nitrogen-rich upper atmosphere of Titan. The atomic species are widely observed in the diffuse region of the ISM, while the presence of aromatic molecules and ions has been confirmed in the dense clouds of the ISM.[60] At the edges between diffuse and dense regions, the reactions described in this paper are relevant.[61] The neutral products H_2O, CO, and CO_2 are generated from the reactions of O atoms with deprotonated toluene, phenol,
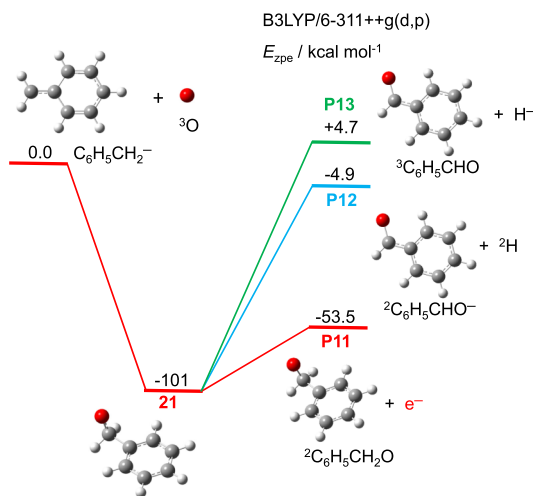
FIG. 6. Potential energy surfaces for the reaction of benzyl ($C_6H_5CH_2^-$) with O on the triplet surfaces. The profiles are plotted for zero-point vibration corrected energies (E_{zpe}, kcal mol^{-1}) relative to the energy of the triplet entrance channel. The intermediates and transition states are denoted in bold as **n** and the products are denoted in bold as **Pn**.

and aniline (Table I). These neutral products are common interstellar species and have been widely detected in the ISM.

The thermal energy reaction rate constants sometimes change with temperature. Unfortunately, most rate constants have been measured near 300 K, not at the very cold temperatures of Titan or of interstellar space. However, temperature-variable experiments have often demonstrated either a simple temperature dependence or no dependence at all.[61] Experimental and theoretical studies of the temperature-dependent reaction rate constants for these systems are excellent future targets.

CONCLUSION

We studied the gas-phase reactions of the anions of deprotonated toluene, aniline, and phenol with N and O atoms experimentally and computationally. The benzyl and anilinide anions react with N atoms exclusively by associative electron detachment. With O atoms, the benzyl and anilinide anions show primarily AED, but minor ionic pathways are also observed; our computation shows that these ionic products can be directly formed on the triplet PES without overall barriers. The phenoxide anion shows dramatically different behavior. There is no measurable reaction with N atom, and ionic product channels dominate in reaction with O atom. This reactivity is distinct from other reaction systems of O atom with aromatic anions. However, DFT calculations confirm this preference for ionic products rather than AED. These computations also show that the formation processes of $C_5H_5^- + CO_2$ and $C_4H_5^- + 2$ CO are spin forbidden but can still occur on the singlet PES via a crossing point between the triplet and singlet PES. These reactions provide important information regarding the chemical processing of atomic and ionic species in the boundary layers between diffuse and dense interstellar clouds as well as in the atmospheres of Titan and the early Earth.

[1]V. Vuitton, R. V. Yelle, and V. G. Anicich, Astrophys. J. **647**, L175–L178 (2006).
[2]J. H. Waite, Jr., D. T. Young, T. E. Cravens, A. J. Coates, F. J. Crary, B. Magee, and J. Westlake, Science **316**, 870–875 (2007).
[3]V. Vuitton, P. Lavvas, R. V. Yelle, M. Galand, A. Wellbrock, G. R. Lewis, A. J. Coates, and J. E. Wahlund, Planet. Space Sci. **57**, 1558–1572 (2009).
[4]N. J. Demarais, Z. Yang, T. P. Snow, and V. M. Bierbaum, Struct. Chem. **24**, 1957–1963 (2013).
[5]V. Vuitton, R. V. Yelle, and M. J. McEwan, Icarus **191**, 722–742 (2007).
[6]P. Lavvas, R. V. Yelle, T. Koskinen, A. Bazin, V. Vuitton, E. Vigren, M. Galand, A. Wellbrock, A. J. Coates, J. E. Wahlund, F. J. Crary, and D. Snowden, Proc. Natl. Acad. Sci. U. S. A. **110**, 2729–2734 (2013).
[7]T. Gautier, N. Carrasco, A. Buch, C. Szopa, E. Sciamma-O'Brien, and G. Cernogora, Icarus **213**, 625–635 (2011).
[8]E. H. Wilson and S. K. Atreya, J. Phys. Chem. A **113**, 11221–11226 (2009).
[9]A. Coustenis and M. Hirtzig, Res. Astron. Astrophys. **9**, 249–268 (2009).
[10]V. Vuitton, R. V. Yelle, and J. Cui, J. Geophys. Res.: Planets **113**, E05007, doi:10.1029/2007JE002997 (2008).
[11]J. H. Waite, H. Niemann, R. V. Yelle, W. T. Kasprzak, T. E. Cravens, J. G. Luhmann, R. L. McNutt, W. H. Ip, D. Gell, V. De La Haye, I. Muller-Wordag, B. Magee, N. Borggren, S. Ledvina, G. Fletcher, E. Walter, R. Miller, S. Scherer, R. Thorpe, J. Xu, B. Block, and K. Arnett, Science **308**, 982–986 (2005).
[12]D. T. Young, J. J. Berthelier, M. Blanc, J. L. Burch, A. J. Coates, R. Goldstein, M. Grande, T. W. Hill, R. E. Johnson, V. Kelha, D. J. McComas, E. C. Sittler, K. R. Svenes, K. Szego, P. Tanskanen, K. Ahola, D. Anderson, S. Bakshi, R. A. Baragiola, L. Barraclough, R. K. Black, S. Bolton, T. Booker, R. Bowman, P. Casey, F. J. Crary, D. Delapp, G. Dirks, N. Eaker, H. Funsten, J. D. Furman, J. T. Gosling, H. Hannula, C. Holmlund, H. Huomo, J. M. Illiano, P. Jensen, M. A. Johnson, D. R. Linder, T. Luntama, S. Maurice, K. P. McCabe, K. Mursula, B. T. Narheim, J. E. Nordholt, A. Preece, J. Rudzki, A. Ruitberg, K. Smith, S. Szalai, M. F. Thomsen, K. Viherkanto, J. Vilppola, T. Vollmer, T. E. Wahl, M. Wuest, T. Ylikorpi, and C. Zinsmeyer, Space Sci. Rev. **114**, 1–112 (2004).
[13]S. Atreya, Science **316**, 843–845 (2007).
[14]A. A. Pavlov, M. T. Hurtgen, J. F. Kasting, and M. A. Arthur, Geology **31**, 87–90 (2003).
[15]O. Shebanits, J. E. Wahlund, K. Mandt, K. Agren, N. J. T. Edberg, and J. H. Waite, Planet. Space Sci. **84**, 153–162 (2013).
[16]A. Wellbrock, A. J. Coates, G. H. Jones, G. R. Lewis, and J. H. Waite, Geophys. Res. Lett. **40**, 4481–4485, doi:10.1002/grl.50751 (2013).
[17]K. Agren, N. J. T. Edberg, and J. E. Wahlund, Geophys. Res. Lett. **39**, L10201, doi:10.1029/2012GL051714 (2012).
[18]A. J. Coates, A. Wellbrock, G. R. Lewis, G. H. Jones, D. T. Young, F. J. Crary, and J. H. Waite, Planet. Space Sci. **57**, 1866–1871 (2009).
[19]M. Agundez, J. Cernicharo, M. Guelin, C. Kahane, E. Roueff, J. Klos, F. J. Aoiz, F. Lique, N. Marcelino, J. R. Goicoechea, M. G. Garcia, C. A. Gottlieb, M. C. McCarthy, and P. Thaddeus, Astron. Astrophys. **517**, L2 (2010).
[20]J. Cernicharo, M. Guelin, M. Agundez, K. Kawaguchi, M. McCarthy, and P. Thaddeus, Astron. Astrophys. **467**, L37–L40 (2007).
[21]M. C. McCarthy, C. A. Gottlieb, H. Gupta, and P. Thaddeus, Astrophys. J. **652**, L141–L144 (2006).
[22]S. Brunken, H. Gupta, C. A. Gottlieb, M. C. McCarthy, and P. Thaddeus, Astrophys. J. **664**, L43–L46 (2007).
[23]J. Cernicharo, M. Guelin, M. Agundez, M. C. McCarthy, and P. Thaddeus, Astrophys. J., Lett. **688**, L83–L86 (2008).
[24]P. Thaddeus, C. A. Gottlieb, H. Gupta, S. Bruenken, M. C. McCarthy, M. Agundez, M. Guelin, and J. Cernicharo, Astrophys. J. **677**, 1132–1139 (2008).
[25]E. Herbst, Nature **289**, 656–657 (1981).
[26]E. Herbst and E. F. van Dishoeck, Annu. Rev. Astron. Astrophys. **47**, 427–480 (2009).
[27]E. Herbst, Chem. Soc. Rev. **30**, 168–176 (2001).
[28]T. P. Snow, V. Le Page, Y. Keheyan, and V. M. Bierbaum, Nature **391**, 259–260 (1998).

[29]D. K. Bohme, Chem. Rev. **92**, 1487–1508 (1992).

[30]A. Candian and P. J. Sarre, Mon. Not. R. Astron. Soc. **448**, 2960–2970 (2015).

[31]M. Tian, B. S. Liu, M. Hammonds, N. Wang, P. J. Sarre, and A. S. C. Cheung, Phys. Chem. Chem. Phys. **14**, 6603–6610 (2012).

[32]G. B. I. Scott, D. A. Fairley, D. B. Milligan, C. G. Freeman, and M. J. McEwan, J. Phys. Chem. A **103**, 7470–7473 (1999).

[33]Z. Yang, B. Eichelberger, O. Martinez, Jr., M. Stepanovic, T. P. Snow, and V. M. Bierbaum, J. Am. Chem. Soc. **132**, 5812–5819 (2010).

[34]B. Eichelberger, T. P. Snow, C. Barckholtz, and V. M. Bierbaum, Astrophys. J. **667**, 1283–1289 (2007).

[35]Z.-C. Wang, C. A. Cole, N. J. Demarais, T. P. Snow, and V. M. Bierbaum, J. Am. Chem. Soc. **137**, 10700–10709 (2015).

[36]C. A. Cole, Z.-C. Wang, T. P. Snow, and V. M. Bierbaum, Astrophys. J. **812**, 77 (2015).

[37]J. M. Van Doren, S. E. Barlow, C. H. DePuy, and V. M. Bierbaum, Int. J. Mass Spectrom. Ion Processes **81**, 85–100 (1987).

[38]V. M. Bierbaum, Int. J. Mass Spectrom. **377**, 456–466 (2015).

[39]N. J. Demarais, Z. B. Yang, T. P. Snow, and V. M. Bierbaum, Astrophys. J. **784**, 25 (2014).

[40]D. L. Thomsen, J. N. Reece, C. M. Nichols, S. Hammerum, and V. M. Bierbaum, J. Am. Chem. Soc. **135**, 15508–15514 (2013).

[41]C. M. Nichols, Z. Yang, and V. M. Bierbaum, Int. J. Mass Spectrom. **353**, 1–6 (2013).

[42]J. M. Garver, Z. Yang, C. M. Nichols, B. B. Worker, S. Gronert, and V. M. Bierbaum, Int. J. Mass Spectrom. **316**, 244–250 (2012).

[43]Z. Yang, C. A. Cole, O. Martinez, Jr., M. Y. Carpenter, T. P. Snow, and V. M. Bierbaum, Astrophys. J. **739**, 19 (2011).

[44]O. Martinez, J. C. Sanchez, S. G. Ard, A. Y. Li, J. J. Melko, N. S. Shuman, H. Guo, and A. A. Viggiano, J. Chem. Phys. **142**, 54305 (2015).

[45]R. M. Cox, J. Kim, P. B. Armentrout, J. Bartlett, R. A. VanGundy, M. C. Heaven, S. G. Ard, J. J. Melko, N. S. Shuman, and A. A. Viggiano, J. Chem. Phys. **142**, 134307 (2015).

[46]A. A. Viggiano, F. C. Fehsenfeld, H. Villinger, E. Alge, and W. Lindinger, Int. J. Mass Spectrom. **39**, 1–8 (1981).

[47]M. J. Frisch, G. W. Trucks, H. B. Schlegel, G. E. Scuseria, M. A. Robb, J. R. Cheeseman, G. Scalmani, V. Barone, B. Mennucci, G. A. Petersson, H. Nakatsuji, M. Caricato, X. Li, H. P. Hratchian, A. F. Izmaylov, J. Bloino, G. Zheng, J. L. Sonnenberg, M. Hada, M. Ehara, K. Toyota, R. Fukuda, J. Hasegawa, M. Ishida, T. Nakajima, Y. Honda, O. Kitao, H. Nakai, T. Vreven, J. A. Montgomery, Jr., J. E. Peralta, F. Ogliaro, M. Bearpark, J. J. Heyd, E. Brothers, K. N. Kudin, V. N. Staroverov, R. Kobayashi, J. Normand, K. Raghavachari, A. Rendell, J. C. Burant, S. S. Iyengar, J. Tomasi, M. Cossi, N. Rega, J. M. Millam, M. Klene, J. E. Knox, J. B. Cross, V. Bakken, C. Adamo, J. Jaramillo, R. Gomperts, R. E. Stratmann, O. Yazyev, A. J. Austin, R. Cammi, C. Pomelli, J. W. Ochterski, R. L. Martin, K. Morokuma, V. G. Zakrzewski, G. A. Voth, P. Salvador, J. J. Dannenberg, S. Dapprich, A. D. Daniels, Ö. Farkas, J. B. Foresman, J. V. Ortiz, J. Cioslowski, and D. J. Fox, GAUSSIAN 09, Revision C.01, Gaussian, Inc., Wallingford, CT, 2009.

[48]H. B. Schlegel, J. Comput. Chem. **3**, 214–218 (1982).

[49]C. Peng, P. Y. Ayala, H. B. Schlegel, and M. J. Frisch, J. Comput. Chem. **17**, 49–56 (1996).

[50]C. Gonzalez and H. B. Schlegel, J. Chem. Phys. **90**, 2154–2161 (1989).

[51]C. Gonzalez and H. B. Schlegel, J. Phys. Chem. **94**, 5523–5527 (1990).

[52]C. T. Lee, W. T. Yang, and R. G. Parr, Phys. Rev. B: Condens. Matter Mater. Phys. **37**, 785–789 (1988).

[53]W. J. Hehre, R. Ditchfield, and J. A. Pople, J. Chem. Phys. **56**, 2257–2261 (1972).

[54]T. Clark, J. Chandrasekhar, G. W. Spitznagel, and P. V. R. Schleyer, J. Comput. Chem. **4**, 294–301 (1983).

[55]A. Ricca, C. W. Bauschlicher, Jr., and E. L. O. Bakes, Icarus **154**, 516–521 (2001).

[56]A. Ricca, C. W. Bauschlicher, and M. Rosi, Chem. Phys. Lett. **347**, 473–480 (2001).

[57]A. Buonaugurio, X. Zhang, S. T. Stokes, Y. Wang, G. B. Ellison, and K. H. Bowen, Int. J. Mass Spectrom. **377**, 278–280 (2015).

[58]J. P. Lebreton, A. Coustenis, J. Lunine, F. Raulin, T. Owen, and D. Strobel, Astron. Astrophy. Rev. **17**, 149–179 (2009).

[59]J. H. Waite, D. T. Young, A. J. Coates, F. J. Crary, B. A. Magee, K. E. Mandt, and J. H. Westlake, in *IAU: Organic Matter in Space*, edited by S. Kwok and S. Sandford (Proceedings IAU Symposium No. 251, 2008), pp. 321–326.

[60]P. Caselli, C. M. Walmsley, R. Terzieva, and E. Herbst, Astrophys. J. **499**, 234–249 (1998).

[61]T. P. Snow and V. M. Bierbaum, Annu. Rev. Anal. Chem. **1**, 229–259 (2008).